Anti-inflammatory Potential of Endophytic Chaetomium globosum from Drynaria quercifolia: *In Vitro* Evaluation and *In silico* Investigation of NF-Kb signalling Modulation

Swetha R[1], Sandhiya Viswanathan[2], Pushpalingam K[3], B. Kirthiga[4*]

[1]Research Scholar, PG & Research Department of Microbiology, Dwaraka Doss Goverdhan Doss Vaishnav College, Chennai, Tamil Nadu, India – 600106.
E mail: swethapandian.r@gmail.com

[2]Research Scientist, School of Biotechnology, Kalinga Institute of Industrial Technology (KIIT) Deemed to be University, Bhubaneswar - 751024, Odisha, 600013.
E mail: ssandia12@gmail.com

[3]Research Scholar, PG & Research Department of Microbiology, Dwaraka Doss Goverdhan Doss Vaishnav College, Chennai, Tamil Nadu, India – 600106
E mail: lplingam1200@gmail.com

[4]Associate Professor, PG & Research Department of Microbiology, Dwaraka Doss Goverdhan Doss Vaishnav College, Chennai, Tamil Nadu, India – 600106
E mail: kirthiga@dgvaishnavcollege.edu.in

* Corresponding author: B. Kirthiga
E mail: kirthiga@dgvaishnavcollege.edu.in

ABSTRACT

Endophytic fungi inhabiting medicinal plants are recognized as prolific producers of bioactive secondary metabolites with diverse pharmacological activities. However, the anti-inflammatory potential of endophytic fungi associated with *Drynaria quercifolia* remains largely unexplored. In the present study, endophytic fungi isolated from *Drynaria quercifolia* were investigated for their anti-inflammatory potential through integrated *in vitro*, *in silico* assessments. A total of seventeen endophytic fungal isolates were recovered and screened for antibacterial activity, of which six active isolates were selected for further analysis. Among these, isolate SK04 exhibited the highest anti-inflammatory activity, showing 72.63% inhibition of albumin denaturation and 69.14% inhibition in the HRBC membrane stabilization assay in the ethyl acetate extract. Based on ITS rRNA gene sequencing, SK04 was identified as *Chaetomium globosum*. The ethyl acetate extract of SK04 also exhibited significant concentration-dependent antioxidant activity, with maximum radical scavenging activities of 74.9%, 78.0%, and 68.3% in the DPPH, ABTS, and H_2O_2 assays, respectively, at 200 µg/mL. GC–MS analysis revealed twenty metabolites, among which catechol and 2,4-di-tert-butylphenol were selected for molecular docking studies. Both compounds exhibited favorable binding interactions with proteins involved in the NF-κB Pathway Proteins. Cytotoxicity assessment against Vero cells revealed low toxicity, with cell viability remaining above 85% at all tested concentrations. These findings highlight the potential of *Chaetomium globosum* as a source of anti-inflammatory metabolites and pave the way for future investigations into their pharmacological applications.

KEYWORDS: *Drynaria quercifolia*, endophytic fungi, *Chaetomium globosum*, anti-inflammatory activity, antioxidant activity, GC–MS, molecular docking, cytotoxicity.

How to cite this article: Swetha R, Viswanathan S, Pushpalingam K, Kirthiga B. Anti-inflammatory Potential of Endophytic Chaetomium globosum from Drynaria quercifolia: In Vitro Evaluation and In silico Investigation of NF-κB Signalling Modulation. Int J Drug Deliv Technol. 2026;16(70s): 667-687. DOI: 10.25258/ijddt.16.70s.69

1. INTRODUCTION

The rising prevalence of chronic inflammatory diseases has intensified worldwide concern owing to their significant impact on global health. Persistent or dysregulated inflammatory responses are now considered key contributors to the initiation and progression of several chronic disorders, including cardiovascular diseases, diabetes mellitus, neurodegenerative diseases, autoimmune disorders, chronic respiratory diseases, cancer, and osteoarthritis (Furman *et al*., 2019). The management of inflammatory conditions mainly relies on steroidal and non-steroidal anti-inflammatory drugs (NSAIDs), which are widely used as first-line therapeutic agents owing to their ability to inhibit cyclooxygenase (COX) enzymes and reduce prostaglandin synthesis involved in the inflammatory response (Machado *et al*., 2021). Despite their therapeutic benefits, prolonged use of these drugs may cause adverse effects, including gastrointestinal irritation, nephrotoxicity, hepatotoxicity, and cardiovascular complications (Ghlichloo & Gerriets, 2023). This has led to increasing interest in identifying natural anti-

inflammatory agents from diverse biological resources.

Medicinal plants have long served as valuable sources of bioactive compounds with therapeutic potential, and medicinal ferns are traditionally used for the treatment of various ailments. *Drynaria quercifolia* (L.) J. Sm. is a widely used medicinal fern belonging to the family Polypodiaceae and distributed in Bangladesh, India, Pakistan, North America, and Africa (Ahmed *et al*., 2015). The fertile fronds and rhizomes of *D. quercifolia* have been traditionally employed for the treatment of swellings, rheumatic complaints, bone fractures, diarrhea, typhoid, cholera, jaundice, fever, headache, and skin diseases (Anuja *et al*., 2014; Modak *et al*., 2021). Recent studies have further demonstrated its antioxidant, antimicrobial, anti-inflammatory, anti-arthritic, hepatoprotective, and wound-healing activities (Deepa *et al*., 2025). The therapeutic potential of medicinal plants may also be influenced by their associated endophytic fungi, which are recognized as prolific producers of diverse bioactive secondary metabolites. As integral components of the plant microbiome, these fungi are increasingly explored for their potential pharmaceutical applications (Alam *et al*., 2021). However, the anti-inflammatory potential of endophytic fungi associated with *Drynaria quercifolia* remains largely unexplored.

The present study aimed to isolate endophytic fungi from *Drynaria quercifolia* and evaluate their anti-inflammatory potential. The most active isolate was further explored to characterize its bioactive profile and to obtain preliminary insights into the molecular basis underlying its anti-inflammatory effects.

2. METHODOLOGY

2.1 Study area and plant collection

Healthy plants of *Drynaria quercifolia* (L.) J. Sm. (Polypodiaceae) were collected during the monsoon season from Chitteri Hills, Kodaikanal Hills, Kolli Hills, and Yelagiri Hills, Tamil Nadu, India. The collected plants were taxonomically identified and authenticated by the Regional Research Institute of Unani Medicine (RRIUM), Chennai, India. Healthy rhizomes, fronds, stems, and roots were selected for the isolation of endophytic fungi.

2.2 Isolation of Fungal Endophytes

Plant tissues were surface sterilized according to Deepak and Virk (2022) with slight modifications. Sterilized segments were inoculated onto water agar (WA) supplemented with amoxicillin (50 mg/L) to prevent contamination. Emerging fungal colonies were purified on Potato Dextrose Agar (PDA) plates and Colonization frequency (CF%) was calculated as follows:

$$\text{Colonization Frequency (CF\%)} = \frac{\text{Number of colonized segments}}{\text{Total number of segments placed}} \times 100.$$

The isolates were identified using lactophenol cotton blue staining based on morphological characteristics.

2.3 Primary Screening of Endophytic Fungal Isolates

Endophytic fungal isolates were screened for antibacterial activity against inflammation-associated bacterial pathogens, namely *Staphylococcus aureus* (MTCC 96), *Streptococcus pyogenes* (MTCC 1925), *Klebsiella pneumoniae* (MTCC 109), and *Pseudomonas aeruginosa* (MTCC 424), obtained from MTCC, Chandigarh, India, using an agar plug assay. Mueller–Hinton agar plates were uniformly swabbed with the bacterial cultures, and 6 mm agar plugs of actively growing fungal colonies (SK01–SK17) were placed onto the seeded plates and incubated at 37°C for 24 h. Antibacterial activity was assessed by measuring the inhibition zones (mm).

2.4 Production of secondary metabolites

Six endophytic fungal isolates (SK01, SK02, SK04, SK10, SK14, and SK16) exhibiting antibacterial activity against all tested pathogens were selected for secondary metabolite production with slight modifications of Deshmukh *et al*. (2009) and Song *et al*. (2024). Agar plugs from PDA cultures were inoculated into 100 mL potato dextrose broth (PDB) and incubated at 25°C for 14–21 days under static conditions. The culture filtrate and mycelial mat were extracted thrice with 80% methanol, ethyl acetate, and petroleum ether and concentrated using a rotary evaporator. Extraction yields were expressed as mg/100 mL culture broth.

2.5 *In Vitro* Anti-inflammatory Assay

2.5.1 Protein denaturation assay

The protein denaturation assay was performed according to Moharram et al. (2024) with minor modifications. Crude extracts (100 µg/mL) and diclofenac sodium were separately mixed with 10 mL of 1% bovine serum albumin (BSA) prepared in phosphate-buffered saline (PBS). The pH of the reaction mixture was adjusted to 6.5 and incubated at room temperature for 20 min, followed by heating at 60°C for 15 min. After cooling, absorbance was measured at 660 nm. The percentage inhibition of protein denaturation was calculated as follows:

$$\text{Percentage of inhibition} = \frac{\text{Absorbance of control} - \text{Absorbance of sample}}{\text{Absorbance of control}} \times 100$$

2.5.2 Membrane stabilization assay

The HRBC membrane stabilization assay was performed according to Bhadra and Vasundhara (2024) with slight modifications. Fresh blood collected with informed consent was washed with 0.9% saline, and a 10% (v/v) RBC suspension was prepared in phosphate-buffered saline (PBS, pH 7.4).

Crude extracts (100 µg/mL) were mixed with the RBC suspension and incubated at 37°C for 30 min and 2 ml of hypotonic solution was added to induce hemolysis, followed by incubation at 37°C for 30 min and centrifugation. The absorbance of the supernatant was measured at 560 nm. Diclofenac sodium and distilled water served as the standard and control, respectively. The percentage inhibition of hemolysis was calculated as:

$$\text{Percentage of inhibition} = \frac{\text{Absorbance of control} - \text{Absorbance of sample}}{\text{Absorbance of control}} \times 100$$

Based on its significant inhibitory, the ethyl acetate extract of isolate SK04 was further evaluated for antioxidant activity. Subsequently, isolate SK04 was subjected to partial ITS rRNA gene sequencing for identification.

2.6 Antioxidant activity

2.6.1 DPPH (2,2-diphenyl-1-picrylhydrazyl) radical scavenging activity

The antioxidant potential of the ethyl acetate extract of isolate SK04 was evaluated by the DPPH radical scavenging assay. Different concentrations of the ethyl acetate extract (12.5, 25, 50, 100, and 200 µg/mL) were mixed with DPPH solution (0.06 mmol/L) prepared in methanol and incubated in the dark for 10 min. Absorbance was measured at 517 nm using a microplate reader. L-ascorbic acid was used as the standard, and 10% DMSO served as the control (Gurgel *et al*., 2023). The percentage of DPPH radical scavenging activity was calculated using the following formula

$$\% \text{ of inhibition} = \frac{\text{Absorbance of control} - \text{Absorbance of sample}}{\text{Absorbance of control}} \times 100$$

2.6.2 ABTS (2,2'-azino-bis(3-ethylbenzothiazoline-6-sulfonic acid) assay

The ABTS radical cation (ABTS•+) was prepared by combining equal volumes of 7 mM ABTS solution and 2.4 mM potassium persulfate solution, followed by incubation in the dark for 12 h at room temperature. The resulting radical solution was diluted with ethanol until an absorbance of 0.70 ± 0.01 was obtained at 734 nm. Aliquots (20 µL) of the ethyl acetate extract of isolate SK04 (12.5–200 µg/mL) were mixed with 3 mL of the diluted ABTS•+ solution and incubated in the dark for 6 min. Absorbance was measured at 734 nm using a UV–Visible spectrophotometer. Ethanol and L-ascorbic acid served as the blank and standard, respectively. Radical scavenging activity was calculated as percentage inhibition using the following formula:

$$\% \text{ Scavenging activity} = \frac{\text{Absorbance of control} - \text{Absorbance of sample}}{\text{Absorbance of control}} \times 100$$

2.6.3 Hydrogen peroxide (H2O2) radical scavenging activity assay

A 43 mM H_2O_2 solution was prepared in 0.1 M phosphate buffer (pH 7.4). The ethyl acetate extract of isolate SK04 (12.5–200 µg/mL) was mixed with the H_2O_2 solution and incubated at room temperature for 5 min. Absorbance was measured at 230 nm using a UV–Visible spectrophotometer. Phosphate buffer without H_2O_2 and L-ascorbic acid served as the blank and standard, respectively. The H_2O_2 scavenging activity was calculated using the following formula:

$$\% \ H_2O_2 \text{ scavenging activity} = \frac{\text{Absorbance of control} - \text{Absorbance of sample}}{\text{Absorbance of control}} \times 100$$

2.7 Identification of endophytic fungi

Pure culture of screened endophytic fungal isolate was identified based on morphological characteristics. Molecular identification was performed using ITS rRNA gene sequencing. PCR amplification was carried out using ITS1 and ITS4 primers. The amplified PCR products were sequenced, and the obtained sequences were subjected to BLAST analysis using the NCBI GenBank database to determine sequence homology with closely related fungal strains. A phylogenetic tree was constructed using MEGA 7.0 software.

2.8 GC-MS analysis

GC–MS analysis was performed using a Thermo Scientific Trace GC Ultra coupled with an ISQ single quadrupole mass spectrometer equipped with a TG-5MS capillary column. Helium was used as the carrier gas at a flow rate of 1.0 mL/min. The oven temperature was programmed from 60°C to 280°C at 10°C/min. Electron ionization was carried out at 70 eV with an injection volume of 1 µL. Metabolites were identified by comparing the mass spectra with NIST libraries.

2.9 Cytotoxicity assay

Vero cells were cultured in 96-well plates at a density of 1 × 10^4 cells/well in Dulbecco's Modified Eagle Medium (DMEM) supplemented with 1× antibiotic-antimycotic solution and 10% fetal bovine serum (FBS) and incubated at 37°C under 5% CO_2 until confluence. Upon reaching confluence, cells were washed with 200 µL of 1× PBS and treated with various concentrations of the ethyl acetate extract of isolate SK04 prepared in serum-free medium for 24 h. Subsequently, MTT solution (0.5 mg/mL in 1× PBS) was added to each well and incubated for 4 h at 37°C. The medium was removed, and the resulting formazan crystals were dissolved in 100 µL DMSO. Absorbance was measured at 570 nm using a microplate reader, and cell viability was determined relative to untreated control cells (Shanthi & Saravanan, 2021).

2.10 In-Silico Anti-inflammatory Assessment

2.10.1 Target Protein Preparation

The crystal structures of TLR4–MD2 (PDB ID: 3FXI), IRAK4 (PDB ID: 2NRY), IKKβ (PDB ID: 3RZF), and NF-κB p50/p65 (PDB ID: 1VKX) were retrieved from the RCSB Protein Data Bank (**https://www.rcsb.org**) and prepared using AutoDock Tools 4.2 by removing water molecules, co-crystallized ligands, and DNA chains (1VKX), followed by the addition of polar hydrogen atoms and Kollman charges. The prepared proteins were converted to PDBQT format. Docking regions are summarized in Table 1.

Table 1. Inflammatory target proteins involved in the NF-κB signaling pathway

Protein	PDB ID	Target Region
NF-κB p50/p65	1VKX	DNA-binding interface
IKKβ	3RZF	ATP-binding catalytic pocket
IRAK4	2NRY	ATP-binding catalytic pocket
TLR4–MD2	3FXI	MD-2 hydrophobic pocket

2.10.2 Ligand Selection and Preparation

Compounds identified through GC–MS analysis and reported to possess anti-inflammatory activity were selected for molecular docking studies. The three-dimensional structures of the selected ligands were retrieved from the PubChem database (https://pubchem.ncbi.nlm.nih.gov/) in SDF format. Ligands were prepared using AutoDock 4.2 by adding polar hydrogen atoms, assigning Gasteiger charges, and converting the structures into PDBQT format.

2.10.3 Docking analysis

The grid parameters used for molecular docking are summarized in Table 2. Docking calculations were performed using AutoDock 4.2. Multiple docked conformations were generated for each ligand–protein complex and ranked according to their binding energies (kcal/mol). The best binding poses were selected for interaction analysis using Discovery Studio Visualizer.

Table 2. Grid parameters

Protein	PDB ID	Grid Center (X, Y, Z)	Spacing (Å)
NF-κB p50/p65	1VKX	90, 80, 110	0.685
IKKβ	3RZF	40, 45, 40	0.472
IRAK4	2NRY	60, 120, 52	0.375
TLR4–MD2	3FXI	40, 50, 79	0.375

2.11 Statistical analysis

All experiments were performed in triplicate, and the results are presented as mean ± standard deviation (SD). Statistical analyses and graphical representations were carried out using GraphPad Prism software version 11.0.2 (GraphPad Software, San Diego, CA, USA). Differences among groups were analyzed by one-way analysis of variance (ANOVA) followed by Tukey's multiple comparisons test. A probability value of $P < 0.05$ was considered statistically significant. IC_{50} values were determined from dose-response curves and expressed as the concentration required to achieve 50% radical scavenging activity.

3. RESULT

3.1 Isolation of Endophytic fungi

A total of 17 endophytic fungal isolates were recovered from healthy rhizome, frond and stem tissues of Drynaria quercifolia. The colony frequency of endophytic fungi varied among plant tissues (Fig. 1), with the rhizome exhibiting the highest frequency (58.33%), followed by fronds (33.33%) and stems (8.33%). No growth of endophytic fungi was observed in root tissues. The rhizome harbored a greater frequency of endophytic fungi than the aerial tissues of the host plant.

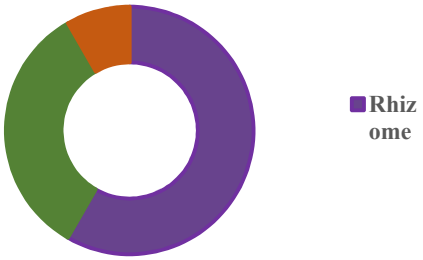

Figure 1: Colony Frequency of Endophytic fungi

The isolated endophytic fungi were identified based on their macromorphological and micromorphological characteristics Table 3. The morphological features of the isolates are presented in Table 4.

Table 3. Morphological Characterization of Endophytic Fungal Isolates

Strain No	Macroscopic view	Microscopic View
SK01		
SK02		
SK03	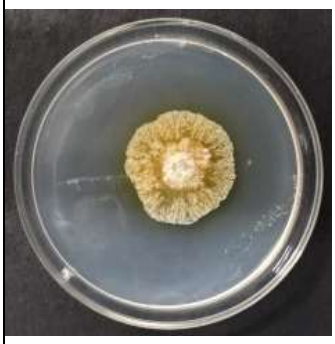	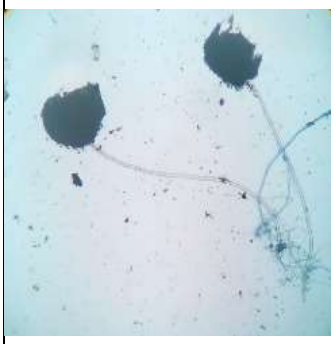

SK04		
SK05		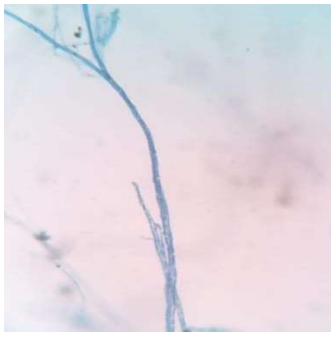
SK06	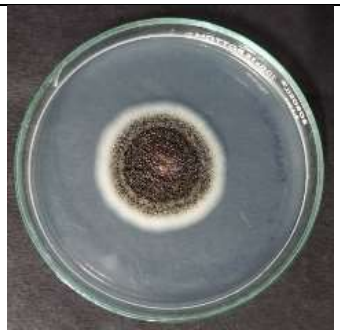	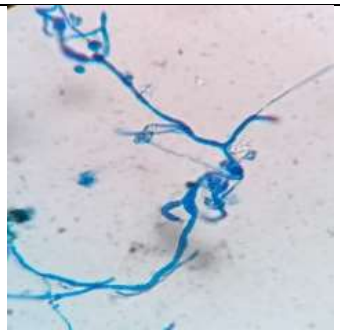

SK07		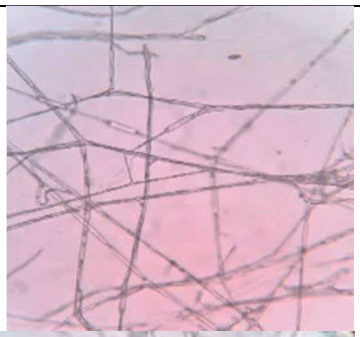
SK08	 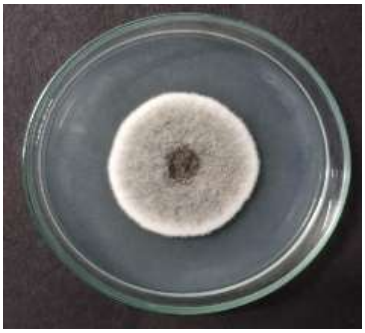	
SK09		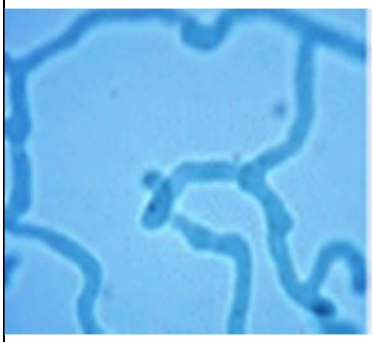

SK10		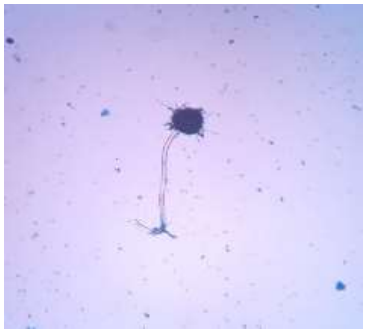
SK11	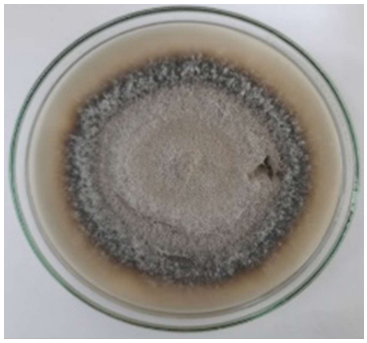	

SK12	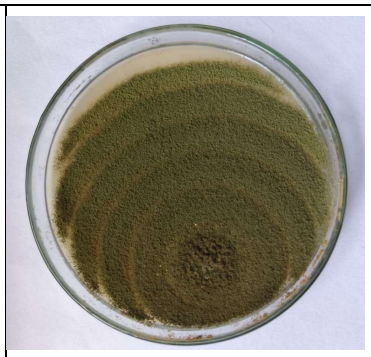	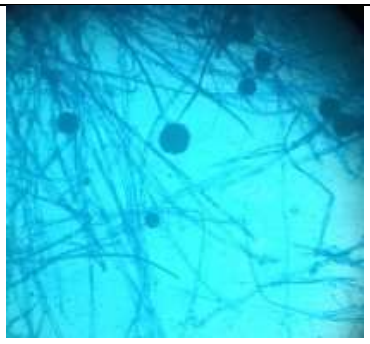

SK13	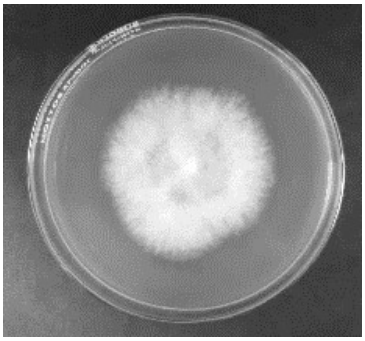	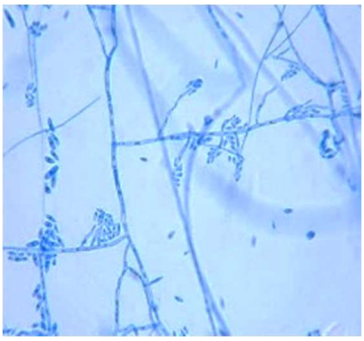
SK14		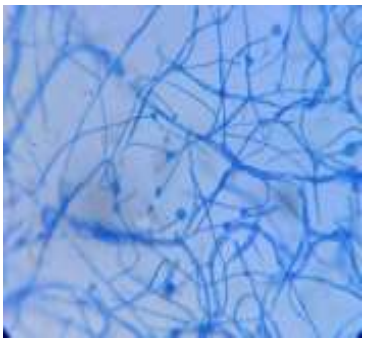
SK15		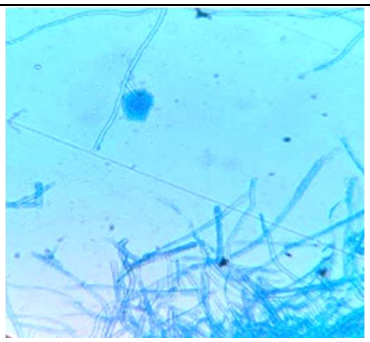

SK16		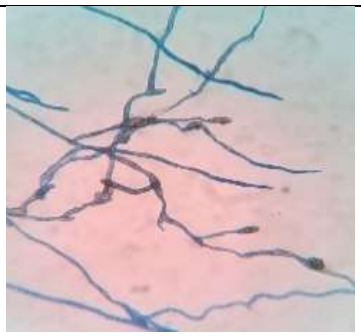
SK17		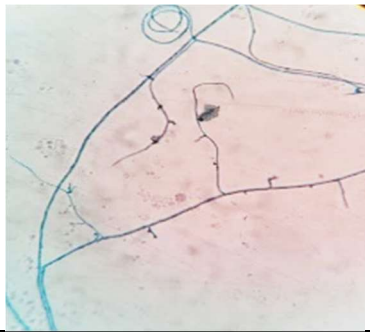

Table. 4 Morphological characterization of endophytic fungal isolates obtained from different parts of D. quercifolia.

Strain No.	**Mycelium Colour**	**Form**	**Elevation**	**Margin**	**Surface Texture**	**Suspected Genera**
SK01	White to orange-pink	Circular	Flat	Entire to undulate	Velvety	*Colletotrichum* sp.
SK02	Grayish black	Circular	Umbonate	Undulate	Velvety to flocose	*Alternaria* sp.
SK03	White to grey becoming black	Circular	Flat to slightly raised	Entire	Cottony to fluffy	*Rhizopus* sp.
SK04	White to grey	Circular	Raised	Entire	Cottony with aerial mycelia	*Chaetomium* sp.
SK05	White to pale	Circular	Flat	Lobate	Cottony	*Colletotrichum* sp.

	orange					
SK06	White becoming grey-black	Circular	Raised	Entire	Suede-like to velvety	*Scedosporium* sp.
SK07	White to grey	Circular	Flat	Filamentous	Cottony	*Pestalotiopsis* sp.
SK08	White becoming green	Irregular	Umbonate	Filiform	Appressed to powdery	*Trichoderma* sp.
SK09	White to cream	Circular	Raised	Entire	Cottony	*Cerato basidium* sp.
SK10	Black	Circular	Flat to slightly raised	Entire	Powdery to granular	*Aspergillus* sp.
SK11	Orange with white hue	Circular	Flat	Lobate	Cottony	*Humicola* sp.
SK12	White becoming green	Circular	Flat to slightly raised	Entire to undulate	Powdery to velvety	*Aspergillus* sp.
SK13	Dark olive green to black	Irregular	Flat	Lobate	Velvety to wrinkled	*Memnoniella* sp.
SK14	White	Circular	Raised	Smooth	Velvety to fluffy	*Phoma* sp.
SK15	Grey to dark brown	Circular	Flat to raised	Entire	Velvety	*Leptosphaeria* sp.
SK16	Dark green to brown	Irregular	Flat	Lobate	Suede-like to downy	*Curvularia* sp.
SK17	White	Circular	Flat	Entire	Sterile cottony mycelium	Sterile mycelia

3.2 Primary screening of endophytic fungi

Antibacterial screening of the 17 endophytic fungal isolates using the agar plug assay revealed that six isolates (SK01, SK02, SK04, SK10, SK14, and SK16) inhibited the growth of all tested bacterial pathogens. The zones of inhibition exhibited by the active isolates are shown in Table 5. These isolates were subsequently selected for metabolite production.

Table 5. Antibacterial activity of endophytic fungal isolates

3.3 Extraction of secondary metabolites

Based on solvent polarity, crude metabolites from the selected endophytic fungal isolates were extracted using petroleum ether, ethyl acetate, and methanol. The extract yield varied among the isolates and solvents employed (Table 6). Ethyl acetate produced comparatively higher yields, with SK04 showing the maximum extract yield, followed by SK01 and SK02, whereas SK10 exhibited the highest yield in petroleum ether.

Table 6. Yield of endophytic fungal crude extracts (mg/100 mL)

Endophytic fungi	**Petroleum ether**	**Ethyl acetate**	**Methanol**
Chaetomium sp. (SK04)	48.6 ± 0.42	111.4 ± 0.76	96.3 ± 0.58
Colletotrichum sp. (SK01)	36.2 ± 0.31	109.7 ± 0.44	88.5 ± 0.63
Alternaria sp. (SK02)	42.8 ± 0.56	109.6 ± 0.82	91.4 ± 0.47
Aspergillus sp. (SK10)	145.4 ± 1.12	52.3 ± 0.36	46.8 ± 0.52

Strain No.	Suspected Genera	S. aureus (mm)	S. pyogenes (mm)	K. pneumoniae (mm)	P. aeruginosa (mm)
SK 01	*Colletotrichum* sp.	4 ± 0.04	5 ± 0.05	2 ± 0.03	3 ± 0.04
SK 02	*Alternaria* sp.	4 ± 0.03	4.7 ± 0.04	2.2 ± 0.05	3.3 ± 0.03
SK 03	*Rhizopus* sp.	–	–	–	–
SK 04	*Chaetomium* sp.	5.4 ± 0.05	4 ± 0.04	2.8 ± 0.03	3.2 ± 0.04
SK 05	*Colletotrichum* sp.	–	–	–	–
SK 06	*Scedosporium* sp.	–	–	–	–
SK 07	*Pestalotiopsis* sp.	2.6 ± 0.03	–	–	–
SK 08	*Trichoderma* sp.	2.2 ± 0.04	–	–	–
SK 09	*Ceratobasidium* sp.	–	–	–	–
SK 10	*Aspergillus* sp.	3.6 ± 0.05	3. ± 0.03	3.4 ± 0.04	3.9 ± 0.05
SK 11	*Humicola* sp.	–	1.1 ± 0.03	–	–
SK 12	*Aspergillus* sp.	–	–	–	–
SK 13	*Memnoniella* sp.	–	–	–	–
SK 14	*Phoma* sp.	1.2 ± 0.04	1.9 ± 0.03	2 ± 0.05	2.6 ± 0.04
SK 15	*Leptosphaeria* sp.	1 ± 0.03	–	–	–
SK 16	*Curvularia* sp.	2 ± 0.04	1.1 ± 0.03	1.2 ± 0.04	3 ± 0.05
SK 17	Sterile mycelia	–	–	–	–
Curvularia sp. (SK16)		58.7 ± 0.67	98.5 ± 0.71	80.6 ± 0.64	
Phoma sp. (SK14)		41.9 ± 0.53	79.2 ± 0.48	74.3 ± 0.55	

3.4 *In-vitro* Anti-inflammatory assays

The inhibitory potential of the selected endophytic fungal extracts against albumin denaturation and HRBC membrane stabilization is depicted in Fig. 4. Ethyl acetate extracts exhibited higher inhibitory activity than petroleum ether and ethanol extracts. Among the isolates, SK04 showed the highest inhibition, with values of 72.63 ± 0.03% in the albumin denaturation assay and 69.14 ± 0.04% in the HRBC membrane stabilization assay. SK01 and SK02 also demonstrated considerable anti-inflammatory activity, whereas SK10 exhibited moderate activity. The lowest inhibitory effects were observed in SK14 and SK16. Overall, SK04 exhibited the highest anti-inflammatory potential among the isolates tested.

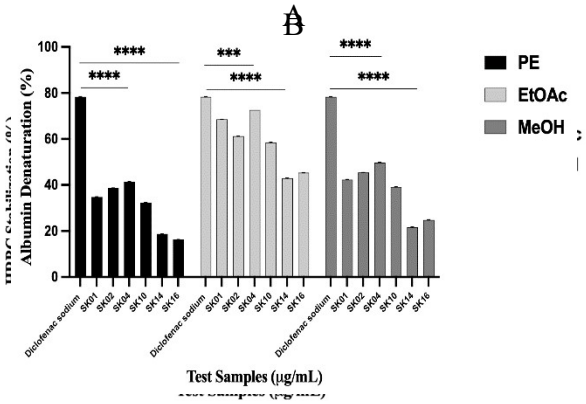

PE – Petroleum ether; EtOAc – Ethyl acetate; MeOH – Methanol. Values are expressed as mean ± SD (n = 3).

Figure 4. Anti-inflammatory activity of selected endophytic fungal extracts determined by (A) albumin denaturation and (B) HRBC membrane stabiliz ation assays

3.5 Antioxidant activity

The antioxidant activity of the ethyl acetate extract of SK04 was evaluated using DPPH, ABTS, and hydrogen peroxide scavenging assays. The extract exhibited concentration-dependent radical scavenging activity (Fig. 5). Maximum inhibition was observed at 200 µg/mL, reaching 74.9 ± 0.7%, 78.0 ± 0.8%, and 68.3 ± 0.7% in the DPPH, ABTS, and hydrogen peroxide scavenging assays, respectively. The IC_{50} values were 44.05 µg/mL for DPPH, 53.85 µg/mL for ABTS, and 74.14 µg/mL for hydrogen peroxide scavenging.

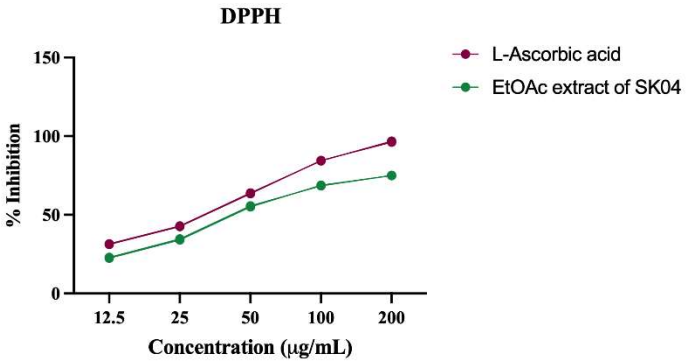

a)

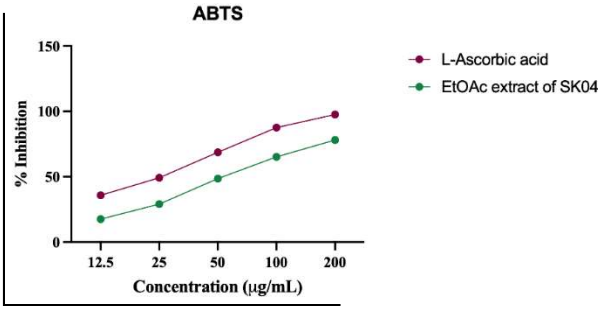

b)

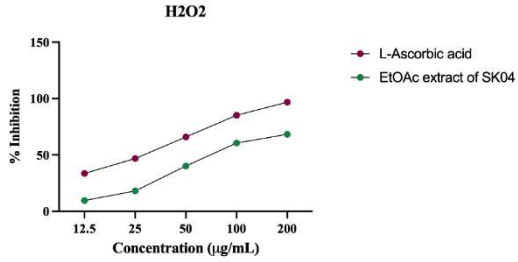

c)

Figure 5. Antioxidant activity of EtOAc extract of SK04 Values are expressed as mean ± SD (n = 3).

Where (**a**) DPPH radical scavenging. (**b**) ABTS radical scavenging. (**c**) H_2O_2 radical scavenging.

3.6 Molecular Identification of SK04

The ITS gene sequence of isolate SK04 was amplified and sequenced. BLAST analysis of the obtained sequence revealed the closest match with *Chaetomium globosum* in the NCBI database. Based on sequence homology and phylogenetic analysis (Fig. 6), isolate SK04 was identified as *Chaetomium globosum*. The sequence was deposited in GenBank under the accession number PV162802.

Figure. 6. Phylogenetic tree of *Chaetomium globosum* strain SK04

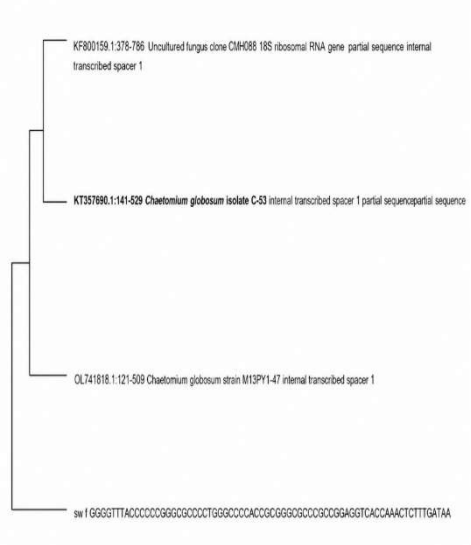

3.7 GC-MS analysis

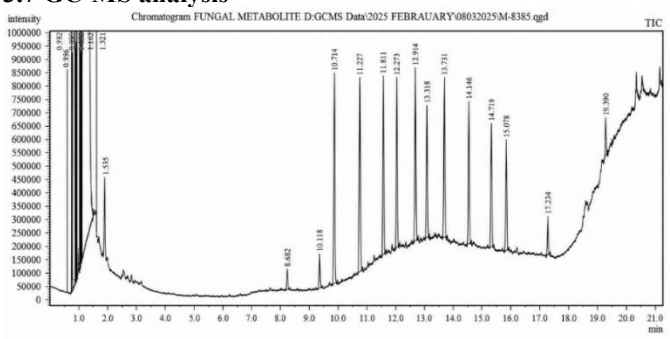

Figure. 7 GC-Ms chromatogram of Ethyl acetate extract of SK04

GC–MS profiling of the fungal extract revealed the presence of 20 compounds, with their retention times and percentage peak areas presented in Table 7 and Fig. 7. Catechol (7.99%) and 2,4-di-tert-butylphenol (8.89%) were selected for molecular docking studies.

Table 7. GC-Ms analysis of EtOAc of SK04

Peak #		R.Time	Area %	Name
1		0.991	16.22	Pentanoic acid, 3-methyl-4-oxo-

2		1.108	11.88	(S)-Methyl 2,3-dihydroxypropanoate
3		1.162	9.07	Ethanol
4		1.227	7.25	Isopropyl Alcohol
5		1.328	10.59	Acetic acid
6		1.535	0.45	Propanoic acid, ethyl ester
7		8.682	0.36	Cyclohexane, (4-methylpentyl)-
8		10.118	0.73	Tetradecane
9		10.714	7.99	Catechol
10		11.227	4.35	Cyclohexane, octyl-
11		11.811	4.08	Z-5-Nonadecene
12		12.273	3.90	Hexadecyl acrylate
13		12.914	8.89	2,4-Di-tert-butylphenol
14		13.318	0.91	8-Octadecanone
15		13.731	3.63	Pentadecanoic acid
16		14.146	2.72	9-Tricosene, (Z)-
17		14.719	2.27	cis-9-Hexadecenal
18		15.078	1.99	n-Tetracosanol-1
19		17.234	1.09	1-Heptacosanol
20		19.390	1.63	1-Heptacosanol

3.8 Cytotoxicity Assay

The MTT assay showed that the ethyl acetate extract of SK04 maintained cell viability above 85% in Vero cells at concentrations up to 500 µg/mL compared with the untreated control. Microscopic observation showed no significant morphological changes in the treated cells. The percentage of cell viability ranged from 95.44% at 30 µg/mL to 85.22% at 500 µg/mL (Fig. 8), suggesting that the extract is less toxic towards Vero cells.

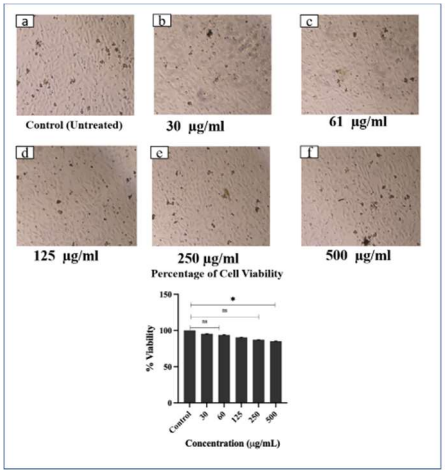

Figure 8. MTT assay of EtOAc crude extract of SK04

3.9 Molecular Docking Analysis of NF-κB Pathway Proteins

Catechol exhibited the highest binding affinity towards TLR4–MD2 (−6.67 kcal/mol), followed by IRAK4 (−6.10 kcal/mol), whereas 2,4-di-tert-butylphenol displayed the strongest interaction with IRAK4 (−7.39 kcal/mol), followed by TLR4–MD2 (−7.15 kcal/mol). Both metabolites exhibited comparatively weaker interactions with IKKβ. Both metabolites exhibited comparatively lower binding affinities towards IKKβ. The docking scores and interaction profiles are presented in Tables 8 and 9, and the binding poses are shown in Figures 9 and 10.

Table 8. Molecular docking of catechol to proteins of the NF-κB pathway

Target Protein	**Binding Energy (kcal/mol)**	**Inhibition constant(µM)**	**Ligand Efficiency**	**Torsional Energy**
NF-κB p65	-5.67	70.0	-0.58	0.60
IKKβ	-4.61	320.0	-0.45	0.60
IRAK4	-6.10	34.0	-0.61	0.60
TLR4–MD2	-6.67	13.0	-0.65	0.60

Table 9. Molecular docking of 2,4-di-tert-butylphenol to proteins of the NF-κB pathway.

Target Protein	**Binding Energy (kcal/mol)**	**Inhibition constant (µM)**	**Ligand Efficiency**	**Torsional Energy**
NF-κB p65	-5.56	84.6	-0.37	0.89
IKKβ	-4.86	275.0	-0.26	0.89
IRAK4	-7.39	3.8	-0.43	0.89
TLR4–MD2	-7.15	5.7	-0.41	0.89

NF-κB p65 (1VKX)

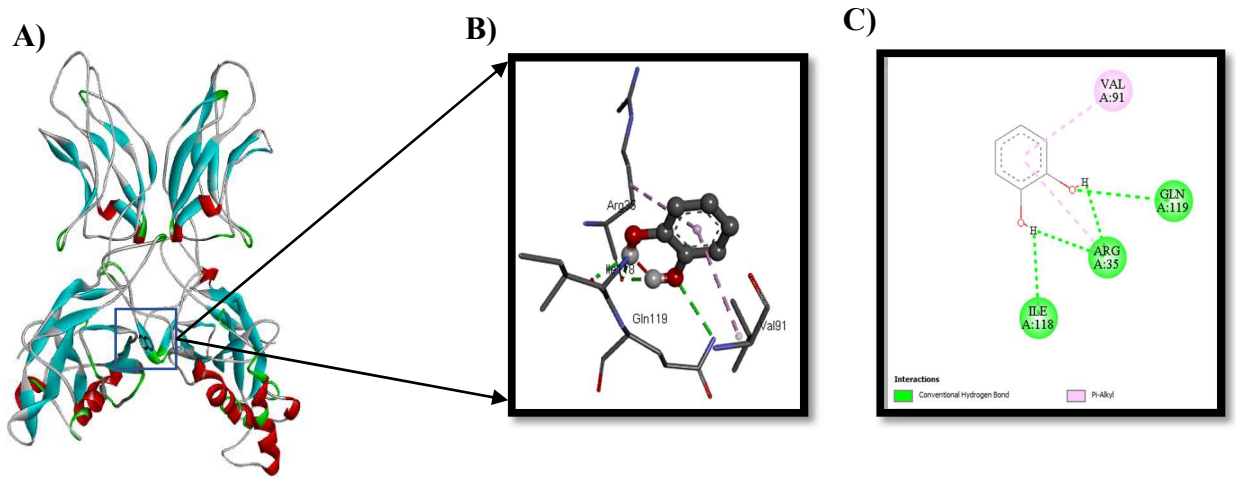

IKKβ (3RZF)IRAK4 (2NRY)

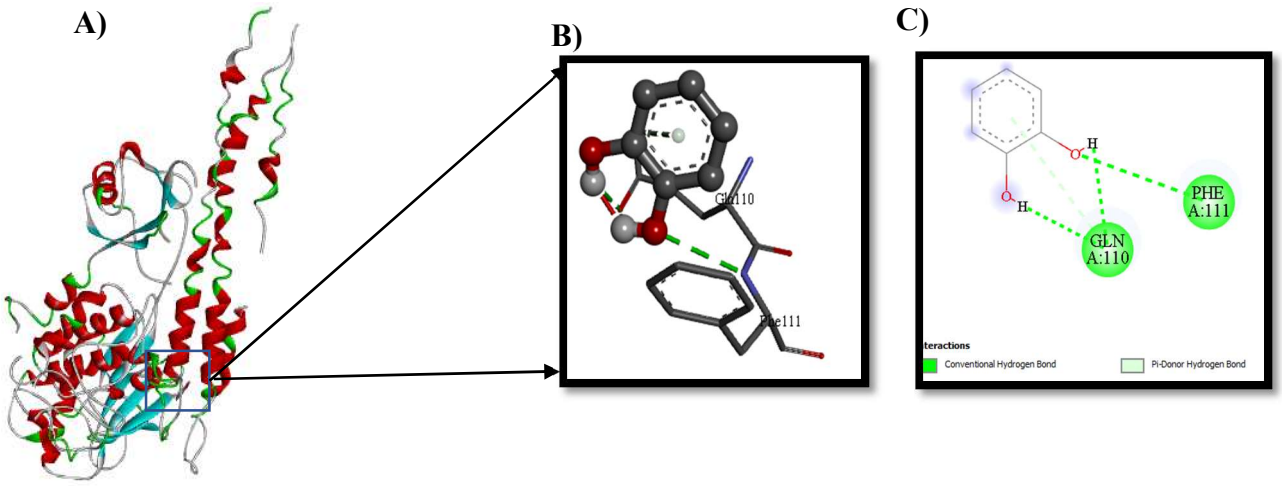

IRAK4 (2NRY)

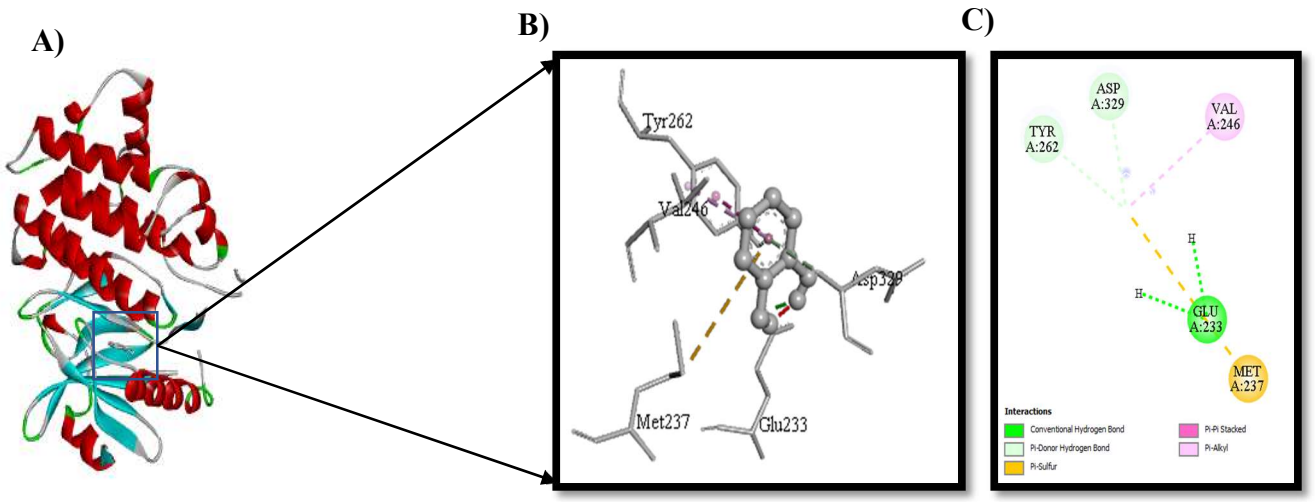

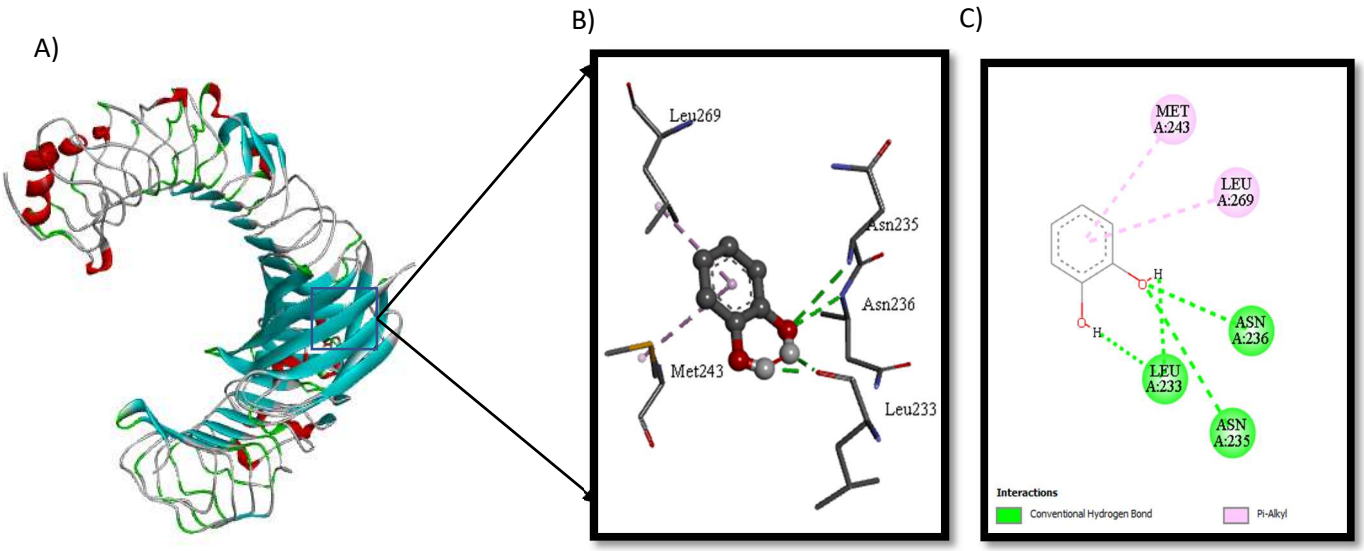

TLR4–MD2 (3FXI)

Figure 9. Molecular docking interactions of catechol with anti-inflammatory target proteins, namely NF-κB p65 (1VKX), IKKβ (3RZF), IRAK4 (2NRY) and TLR4–MD2 (3FXI). For each protein, (A) represents the solid ribbon structure highlighting the ligand-binding region; B) depicts the three-dimensional protein–ligand complexes with interacting residues **(C)** illustrates the two-dimensional interaction map displaying conventional hydrogen bonds (green dotted lines), carbon hydrogen bonds (light green dotted lines), hydrophobic interactions including π-alkyl interactions (light pink dotted lines), π–π stacked interactions (dark pink dotted lines), π-donor hydrogen bonds, and π-sulfur interactions (yellow dotted lines).

NF-κB p65 (1VKX)

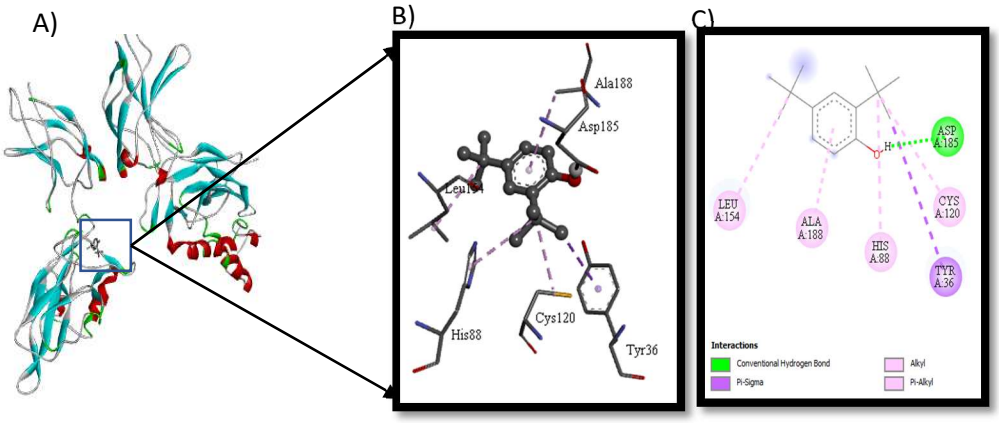

IKKβ (3RZF)

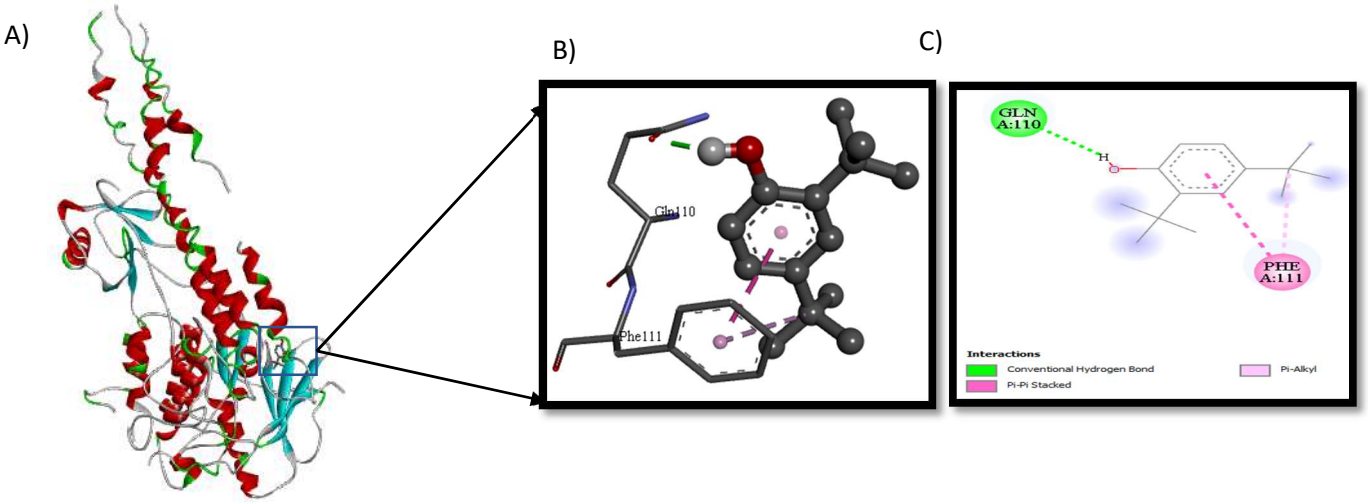

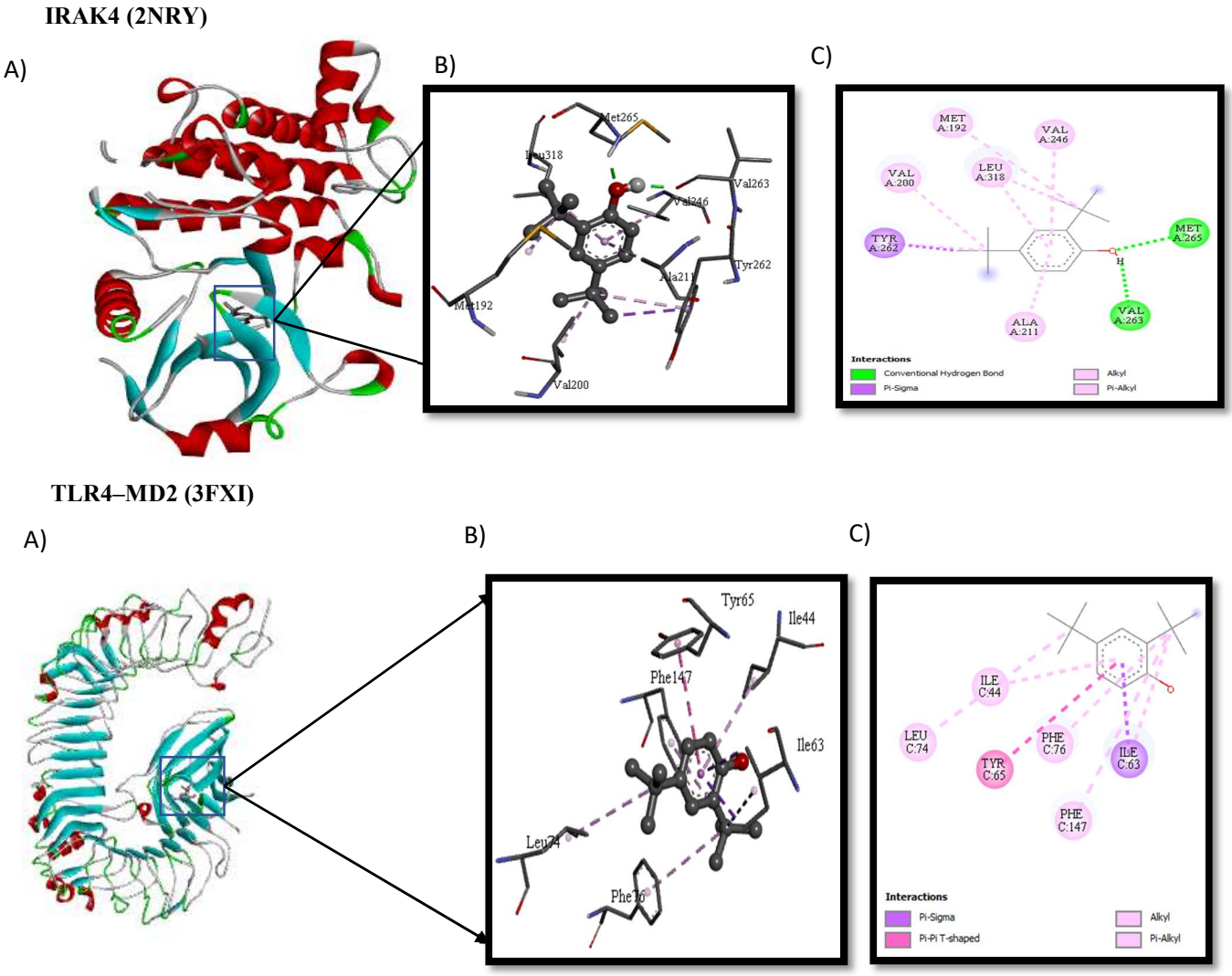

Figure 10. Molecular docking interactions of 2,4-di-tert-butylphenol with anti-inflammatory target proteins, namely NF-κB p65 (1VKX), IKKβ (3RZF), IRAK4 (2NRY), and TLR4–MD2 (3FXI). For each protein, (A) represents the solid ribbon structure highlighting the ligand-binding region; B) depicts the three-dimensional protein–ligand complexes with interacting residues; **(C)** illustrates the two-dimensional interaction map displaying conventional hydrogen bonds (green dotted lines), hydrophobic interactions including alkyl and π-alkyl interactions (light pink dotted lines), π–sigma interactions (purple dotted lines), π–π T-shaped interactions (magenta dotted lines), and π–π stacked interactions (dark pink dotted
lines).

4. DISCUSSION

The present study revealed a diverse community of endophytic fungi associated with Drynaria quercifolia, highlighting the potential of this medicinal fern as a reservoir of bioactive fungal endophytes. A total of seventeen fungal isolates were recovered from different plant tissues, with the highest colonization frequency observed in the rhizomes. Similar tissue-specific colonization patterns have been reported in medicinal plants, where belowground tissues harbor more diverse endophytic fungal communities than aboveground tissues (Zuo *et al*., 2022).

The agar plug diffusion assay revealed that six of the seventeen endophytic fungal isolates exhibited antibacterial activity against all tested bacterial pathogens and were therefore selected for subsequent analyses. Based on their morphological characteristics, these active isolates were tentatively assigned to the genera *Colletotrichum*, *Alternaria*, *Chaetomium*, *Aspergillus*, *Phoma*, and *Curvularia*. Similar observations have been reported in studies of

endophytic fungi associated with medicinal plants, where only a subset of the isolated endophytes demonstrated antimicrobial activity (Santos *et al*., 2015). The observed variation in antibacterial activity among the isolates attributed to differences their capacity to produce bioactive secondary metabolites. Previous studies reported that the antimicrobial potential of microbial isolates is associated with the diversity and abundance of the metabolites they produce (Mazumdar & Thakur, 2024). The broad-spectrum antibacterial activity exhibited by the selected isolates suggests their potential to produce metabolites capable of inhibiting a diverse range of bacterial pathogens, highlighting their promise as sources of antimicrobial compounds.

The extraction yield varied considerably among the solvents employed, with ethyl acetate consistently producing higher yields than petroleum ether and ethanol. Similar observations have been reported for endophytic fungi, where ethyl acetate yielded higher amounts of crude metabolites than other solvent fractions and was considered an effective solvent for recovering fungal secondary metabolites (Nathiya & Mahalingam, 2018). The predominance of the ethyl acetate fraction suggests that the active isolates produce metabolites that are preferentially extracted by moderately polar solvents. The anti-inflammatory activity exhibited by the ethyl acetate extracts further supports the effectiveness of this solvent in recovering biologically active fungal metabolites.

The ethyl acetate extracts of the selected endophytic fungal isolates exhibited anti-inflammatory activity in both the albumin denaturation and HRBC membrane stabilization assays. Among the isolates tested, SK04 exhibited the highest inhibitory activity in both assays. Although its activity was lower than that of the reference drug diclofenac sodium, the observed inhibition suggests the presence of metabolites with anti-inflammatory activity. Protein denaturation is associated with inflammatory responses, and inhibition of this process is widely regarded as an indicator of anti-inflammatory activity (Hasan *et al*., 2023). Therefore, the inhibition of albumin denaturation exhibited by SK04 supports the anti-inflammatory potential of its metabolites. Furthermore, SK04 exhibited substantial membrane stabilization activity in the HRBC assay. As the erythrocyte membrane is considered analogous to the lysosomal membrane, stabilization of erythrocytes indicates the ability of bioactive compounds to prevent the release of inflammatory mediators (Aidoo *et al*., 2021). The anti-inflammatory potential of *Chaetomium globosum* has previously been demonstrated in an experimental arthritis model, where its secondary metabolites reduced inflammatory responses and tissue damage (Abdel-Azeem *et al*., 2016). Although the present study employed *in vitro* protein denaturation and membrane stabilization assays, the anti-inflammatory activity exhibited by SK04 is consistent with these earlier findings and further supports the anti-inflammatory potential of metabolites produced by *C. globosum*.

In addition to its anti-inflammatory activity, the ethyl acetate extract of SK04 exhibited significant antioxidant activity in the DPPH, ABTS, and hydrogen peroxide scavenging assays, with radical scavenging activity increasing in a concentration-dependent manner. Oxidative stress and inflammation are closely interconnected processes, as excessive production of reactive oxygen species (ROS) contributes to cellular damage and promotes inflammatory responses. Antioxidants neutralize these reactive species and help maintain cellular redox balance, thereby reducing oxidative stress-induced tissue injury (Chaudhary *et al*., 2023). The antioxidant activity observed in the present study indicates the presence of bioactive metabolites capable of scavenging free radicals and reducing oxidative damage. Similar antioxidant activity has been reported for *Chaetomium globosum*, in which fungal extracts exhibited notable DPPH and ABTS radical scavenging activities (Kaur *et al*., 2020). The antioxidant activity observed for SK04 is therefore consistent with previous findings and suggests that phenolic constituents and other secondary metabolites capable of donating electrons or hydrogen atoms contribute to its free radical scavenging activity.

Based on its superior anti-inflammatory and antioxidant activities, SK04 was selected for molecular identification. ITS rRNA sequence analysis identified isolate SK04 as *Chaetomium globosum*. This endophytic fungus has been reported as a rich source of bioactive secondary metabolites exhibiting diverse biological activities (Dwibedi *et al*., 2023). To gain further insight into the chemical constituents responsible for the observed bioactivity, the ethyl acetate extract of SK04 was subjected to GC–MS analysis. The analysis revealed the presence of twenty compounds, demonstrating the chemical diversity of metabolites produced by the isolate. Among the identified metabolites, catechol and 2,4-di-tert-butylphenol were selected for further investigation because of their relatively high abundance in the extract and their reported anti-inflammatory activities (Zheng *et al*., 2008; Nair *et al*., 2020). Interestingly, 2,4-di-tert-butylphenol has previously been reported in *Chaetomium globosum* extracts (Kumari *et al*., 2022), whereas catechol has been identified in bioactive extracts of *Drynaria quercifolia* (Modak *et al*., 2021). The occurrence of these compounds in both the endophytic fungus and its host plant indicates similarities in their metabolite profiles, although

whether this reflects independent biosynthesis or metabolic interactions requires further investigation. The presence of these compounds contributes to the anti-inflammatory activity exhibited by SK04. However, the observed bioactivity is likely influenced by the synergistic effects of other metabolites present in the extract. Therefore, catechol and 2,4-di-tert-butylphenol were selected for further investigation to evaluate their potential contribution to the anti-inflammatory activity of SK04. Molecular docking analysis predicted favorable interactions of catechol and 2,4-di-tert-butylphenol with key proteins involved in the NF-κB signaling pathway, which plays a central role in regulating inflammatory responses (Napetschnig & Wu, 2013). In the present study, catechol exhibited the highest binding affinity towards TLR4–MD2, whereas 2,4-di-tert-butylphenol exhibited the strongest interaction with IRAK4. Kadioglu *et al*. (2015) demonstrated that kaempferol exerts anti-inflammatory effects through modulation of the NF-κB signaling pathway. Similarly, the favorable interactions of catechol and 2,4-di-tert-butylphenol with proteins involved in the NF-κB pathway suggest their potential role in regulating inflammatory signaling. Furthermore, the low cytotoxicity exhibited by the extract toward Vero cells supports its potential for further pharmacological investigation. Collectively, the present findings provide evidence for the anti-inflammatory potential of *Chaetomium globosum* SK04 and its secondary metabolites. Nevertheless, further in vivo studies are required to validate these findings and clarify the precise role of these metabolites in modulating NF-κB-mediated inflammatory responses.

5. CONCLUSION

The present study highlights the ethyl acetate extract of *Chaetomium globosum* SK04 as a promising source of metabolites with anti-inflammatory and antioxidant properties. The observed biological activities, together with its low cytotoxicity and the identification of metabolites predicted to exhibit favorable interactions with proteins involved in inflammatory signaling, underscore the pharmacological potential of this fungal extract. These findings reinforce the significance of endophytic fungi associated with medicinal plants as valuable reservoirs of bioactive compounds and support the further exploration of *C. globosum* SK04 as a prospective source of naturally derived anti-inflammatory agents. Future investigations are required to validate the anti-inflammatory efficacy of the identified metabolites and to elucidate their precise role in inflammatory signaling pathways under *in vivo* conditions.

Reference

1. Abdel-Azeem, A. M., Zaki, S. M., Khalil, W. F., Makhlouf, N. A., & Farghaly, L. M. (2016). Anti-rheumatoid activity of secondary metabolites produced by endophytic Chaetomium globosum. Frontiers in Microbiology, 7, 1477.
2. Ahmed, M. N., Gowan, M., Azam, M. N. K., et al. (2015). Clinical appraisals and phytochemical potential of ethnomedicinal pteridophyte: Drynaria quercifolia (L.) J. Smith (Polypodiaceae). Pharmacologyonline.
3. Aidoo, D. B., Konja, D., Henneh, I. T., & Ekor, M. (2021). Protective effect of bergapten against human erythrocyte hemolysis and protein denaturation in vitro. International Journal of Inflammation, 2021, 1279359.
4. Alam, B., Li, J., Ge, Q., Khan, M. A., Gong, J., Mehmood, S., Yuan, Y., & Gong, W. (2021). Endophytic fungi: From symbiosis to secondary metabolite communications or vice versa? Frontiers in Plant Science, 12, 791033.
5. Anuja, G. I., Latha, P. G., Suja, S. R., et al. (2010). Anti-inflammatory and analgesic properties of Drynaria quercifolia (L.) J. Smith. Journal of Ethnopharmacology.
6. Bhadra, F., & Vasundhara, M. (2024). Anti-inflammatory potential of aconitine produced by endophytic fungus Acremonium alternatum. World Journal of Microbiology and Biotechnology, 40(9), 274.
7. Chaudhary, P., Janmeda, P., Docea, A. O., Yeskaliyeva, B., Abdull Razis, A. F., Modu, B., ... & Sharifi-Rad, J. (2023). Oxidative stress, free radicals and antioxidants: Potential crosstalk in the pathophysiology of human diseases. Frontiers in Chemistry, 11, 1158198.
8. Deepa, N., Nirmala, S., Yogalakshmi, T., Udhayakumaran, U., & Velvizhi, K. (2025). Phytochemistry, traditional applications, and therapeutic properties of Drynaria quercifolia. Journal of Pharma Insights and Research, 3(3), 379–391.
9. Deepak, H., & Virk, V. (2022). Optimization of surface sterilization method for the isolation of endophytic fungi associated with Curcuma longa L. and their antibacterial activity. Journal of Advanced Biotechnology and Experimental Therapeutics, 5(2), 334–346.
10. Deshmukh, S. K., Mishra, P. D., Kulkarni-Almeida, A., Verekar, S., Sahoo, M. R., Periyasamy, G., ... & Vishwakarma, R.

(2009). Anti-inflammatory and anticancer activity of ergoflavin isolated from an endophytic fungus. Chemistry & Biodiversity, 6(5), 784–789.
11. Dwibedi, V., Rath, S. K., Jain, S., Martínez-Argueta, N., Prakash, R., Saxena, S., & Rios-Solis, L. (2023). Key insights into secondary metabolites from various Chaetomium species. Applied Microbiology and Biotechnology, 107(4), 1077–1093.
12. Furman, D., Campisi, J., Verdin, E., Carrera-Bastos, P., Targ, S., Franceschi, C., ... & Slavich, G. M. (2019). Chronic inflammation in the etiology of disease across the life span. Nature Medicine, 25(12), 1822–1832.
13. Ghlichloo, I., & Gerriets, V. (2019). Nonsteroidal anti-inflammatory drugs (NSAIDs). StatPearls Publishing.
14. Gurgel, R. S., de Melo Pereira, D. Í., Garcia, A. V. F., Fernandes de Souza, A. T., Mendes da Silva, T., de Andrade, C. P., ... & Albuquerque, P. M. (2023). Antimicrobial and antioxidant activities of endophytic fungi associated with Arrabidaea chica (Bignoniaceae). Journal of Fungi, 9(8), 864.
15. Kadioglu, O., Nass, J., Saeed, M. E. M., Schuler, B., & Efferth, T. (2015). Kaempferol is an anti-inflammatory compound with activity towards NF-κB pathway proteins. Anticancer Research, 35(5), 2645–2650.
16. Kaur, N., Arora, D. S., Kalia, N., & Kaur, M. (2020). Bioactive potential of endophytic fungus Chaetomium globosum and GC–MS analysis of its responsible components. Scientific Reports, 10(1), 18792.
17. Kumari, S., Kumari, S., Attri, C., Sharma, R., Kulshreshtha, S., Benali, T., ... & Sharifi-Rad, J. (2022). GC–MS analysis, antioxidant and antifungal studies of different extracts of Chaetomium globosum isolated from Urginea indica. BioMed Research International, 2022, 1388850.
18. Machado, G. C., Abdel-Shaheed, C., Underwood, M., & Day, R. O. (2021). Non-steroidal anti-inflammatory drugs (NSAIDs) for musculoskeletal pain. BMJ, 372.
19. Mazumdar, R., & Thakur, D. (2024). Antibacterial activity and biosynthetic potential of Streptomyces sp. PBR19 isolated from forest rhizosphere soil of Assam. Brazilian Journal of Microbiology, 55(4), 3335–3352.
20. Modak, D., Paul, S., Sarkar, S., Thakur, S., & Bhattacharjee, S. (2021). Validating potent anti-inflammatory and anti-rheumatoid properties of Drynaria quercifolia rhizome methanolic extract through in vitro, in vivo, in silico and GC-MS-based profiling. BMC Complementary Medicine and Therapies, 21(1), 89.
21. Moharram, A. M., Zohri, A. A., Omar, H. M., & Abd El-Ghani, O. A. (2017). In vitro assessment of antimicrobial and anti-inflammatory potential of endophytic fungal metabolites extracts. European Journal of Biological Research, 7(3), 234–244.
22. Nair, R. V., Jayasree, D. V., Biju, P. G., & Baby, S. (2020). Anti-inflammatory and anticancer activities of erythrodiol-3-acetate and 2,4-di-tert-butylphenol isolated from Humboldtia unijuga. Natural Product Research, 34(16), 2319–2322.
23. Napetschnig, J., & Wu, H. (2013). Molecular basis of NF-κB signaling. Annual Review of Biophysics, 42, 443–468.
24. Nathiya, R., & Mahalingam, G. (2018). Screening and isolation of therapeutic agent for type 2 diabetes mellitus from endophytic fungal metabolites of mangrove plants. Research Journal of Biotechnology, 13.
25. Santos, I. P. D., Silva, L. C. N. D., Silva, M. V. D., Araújo, J. M. D., Cavalcanti, M. D. S., & Lima, V. L. D. M. (2015). Antibacterial activity of endophytic fungi from leaves of Indigofera suffruticosa Miller (Fabaceae). Frontiers in Microbiology, 6, 350.
26. Shanthi, D., & Saravanan, R. (2021). Evaluation of cytotoxicity of normal Vero and anticancer activity of human breast cancer cell lines by aqueous unripe fruit extract of Solanum torvum. Research Journal of Pharmacy and Technology, 14(7), 3504–3508.
27. Song, Z., Sun, Y. J., Xu, S., Li, G., Yuan, C., & Zhou, K. (2023). Secondary metabolites from the endophytic fungus Fusarium decemcellulare F25 and their antifungal activities. Frontiers in Microbiology, 14, 1127971.
28. Zheng, L. T., Ryu, G. M., Kwon, B. M., Lee, W. H., & Suk, K. (2008). Anti-inflammatory effects of catechols in lipopolysaccharide-stimulated microglia cells: Inhibition of microglial neurotoxicity. European Journal of Pharmacology, 588(1), 106–113.
29. Zuo, Y., Hu, Q., Zhang, K., & He, X. (2022). Host and tissue affiliations of culturable endophytic fungi associated with xerophytic plants in the desert region of Northwest China. Agronomy, 12(3), 727.